

UCSF

UC San Francisco Previously Published Works

Title

Direct detection of SARS-CoV-2 RNA using high-contrast pH-sensitive dyes.

Permalink

<https://escholarship.org/uc/item/7qn3k1w5>

Journal

Journal of Biomolecular Techniques, 32(3)

ISSN

1524-0215

Authors

Brown, Timothy A
Schaefer, Katherine S
Tsang, Arthur
et al.

Publication Date

2021-09-01

DOI

10.7171/jbt.21-3203-007

Peer reviewed

Direct detection of SARS-CoV-2 RNA using high-contrast pH-sensitive dyes

Timothy A. Brown,^{1,*} Katherine S. Schaefer,¹ Arthur Tsang,¹ Hyun Ah Yi,¹ Jonathan B. Grimm,¹ Andrew L. Lemire,¹ Fadi M. Jradi,¹ Charles Kim,^{1,†} Kevin McGowan,¹ Kimberly Ritola,¹ Derek T. Armstrong,² Heba H. Mostafa,² Wyatt Korff,¹ Ronald D. Vale,¹ and Luke D. Lavis¹

¹Janelia Research Campus, Howard Hughes Medical Institute, Ashburn, Virginia 20147; and ²Division of Medical Microbiology, Department of Pathology, Johns Hopkins University School of Medicine, Baltimore, Maryland 21287-7093

The worldwide coronavirus disease 2019 pandemic has had devastating effects on health, healthcare infrastructure, social structure, and economics. One of the limiting factors in containing the spread of this virus has been the lack of widespread availability of fast, inexpensive, and reliable methods for testing of individuals. Frequent screening for infected and often asymptomatic people is a cornerstone of pandemic management plans. Here, we introduce 2 pH-sensitive “LAMPshade” dyes as novel readouts in an isothermal Reverse Transcriptase Loop-mediated isothermal AMplification assay for severe acute respiratory syndrome coronavirus 2 RNA. The resulting JaneliaLAMP assay is robust, simple, inexpensive, and has low technical requirements, and we describe its use and performance in direct testing of contrived and clinical samples without RNA extraction.

KEY WORDS: carbofluorescein · LAMPshade · RT-LAMP · Si-fluorescein

INTRODUCTION

In the wake of the coronavirus disease 2019 (COVID-19) pandemic, there has been a significant worldwide effort toward the development of tests that effectively identify severe acute respiratory syndrome coronavirus 2 (SARS-CoV-2)-infected individuals. Management strategies for the COVID-19 outbreak are often centered on the ability to conduct widespread testing for the SARS-CoV-2 virus. Quantitative RT-PCR (qRT-PCR) is the gold-standard assay for virus detection, as it is quantitative, robust, and uses equipment and protocols common in clinical testing laboratories. qRT-PCR assays are best suited for use in centralized testing facilities designed to handle large numbers of patient samples shipped from different sampling locations. This process requires transport logistics, expensive equipment, and technical expertise, however, which can lead to long turnaround times for test results. In addition, reliance on a single assay places pressure on the supply chain for test components, allowing possible disruptions under high demands. Finally, there is a need for more rapid and inexpensive tests that could be applied at point-of-care, near-patient venues or in surveillance testing. To diversify the testing arsenal and to enable alternative testing

modalities, we have developed JaneliaLAMP (jLAMP), a reverse transcriptase (RT)-LAMP assay for the SARS-CoV-2 viral RNA that is inexpensive and simple to perform.

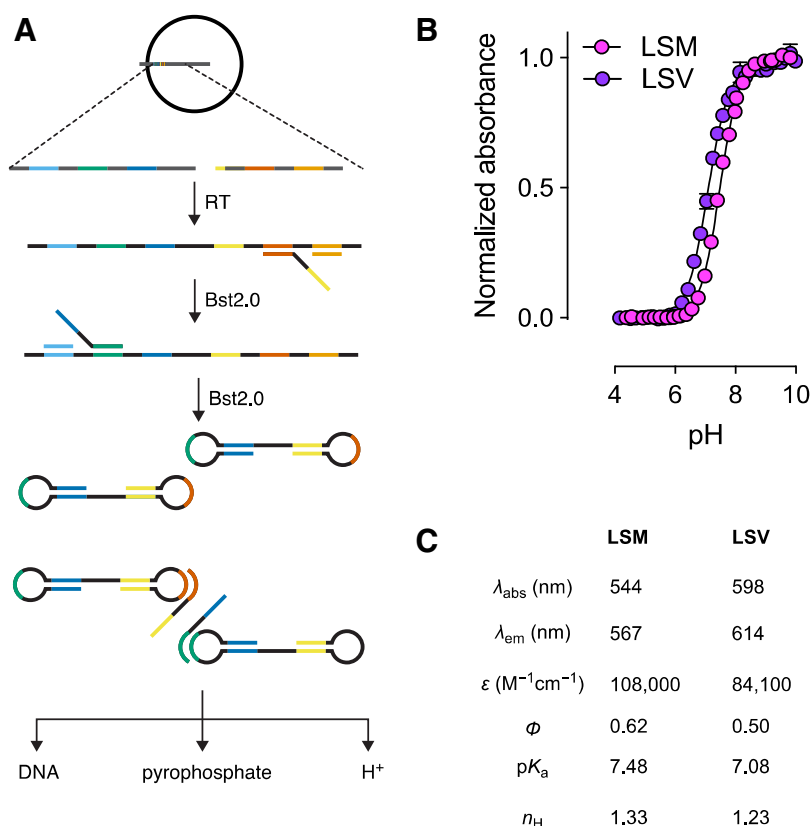
The LAMP technique is an isothermal nucleic acid amplification method developed 20 y ago,¹ and it has been used to detect a variety of human pathogens.² LAMP typically uses a set of 6 primers, which create a dumbbell-shaped single DNA strand with end loops created by self-annealing segments. This substrate is then amplified by other primers using a strand-displacing thermostable DNA polymerase in an isothermal reaction. The method has been adapted to include RT to create the cDNA LAMP template from RNA viruses (Fig. 1A).³ The LAMP reaction produces large amounts of DNA, and a molecule of pyrophosphate and a proton are released for each nucleobase added in the DNA synthesis process (Fig. 1A). All 3 of these LAMP products have been used to determine the progress of the reaction.^{1,4} Protons can be detected by using weakly buffered conditions, which allows a large decrease in pH to accompany DNA synthesis; this can be read out by colorimetric dyes, as pioneered by Tanner *et al.*⁵ Here, we introduce 2 novel high-contrast pH indicators, called “LAMPshade” dyes, and demonstrate their use in jLAMP assays for the detection of SARS-CoV-2 viral RNA. These dyes can be used as both colorimetric and fluorescent readouts. Using inactivated SARS-COV-2 virus and clinical samples, we show that the jLAMP assay does not require RNA extraction, performing well in a direct testing protocol from common viral transport media. We demonstrate sensitivity, specificity, stability, and validation

*ADDRESS CORRESPONDENCE TO: Dr. Timothy A. Brown, Senior Scientist & SciOps Manager, Tool Translation Team, Janelia Research Campus, Howard Hughes Medical Institute, 19700 Helix Drive, Ashburn, VA 20147 (Phone: 571-209-4000; E-mail: brown@janelia.hhmi.org).

†Current address: Sensei Biotherapeutics, Smartlabs, 6 Tide St., Boston, MA 02210, USA.
<https://doi.org/10.7171/jbt.21-3203-007>

FIGURE 1

LAMP and LAMPshade dyes. A) Schematic of LAMP assays for detection of SARS-CoV-2. Bst 2.0 is a strand-displacing DNA polymerase (NEB) (B) pH absorbance/fluorescence response curves. C) Dye photo properties including maximum excitation and emission wavelengths, extinction coefficient, quantum yield, pKa, and Hill coefficient. LSM; LAMPshade Magenta, LSV; LAMPshade Violet



using clinical nasopharyngeal (NP) swab samples and extend the jLAMP protocol to direct testing from saliva.

MATERIALS AND METHODS

LAMPshade dyes

Novel pH indicator dyes were synthesized as previously described: 4,5,6,7-tetrafluoro-Si-fluorescein (LAMPshade Violet) and carbofluorescein (LAMPshade Magenta).^{6,7} We routinely distribute fluorescent dyes and have limited quantities available. Please contact T. Brown or L. Lavis for dye requests. Stock solutions of the LAMPshade dyes were prepared in high-quality DMSO at 1–10 mM and stored at -20°C in DMSO. These were diluted to 2.5 mM or 0.25 mM in nuclease-free water prior to use as $25\times$ working stocks for a final assay concentration of 100 μM and 10 μM , respectively. Frozen stock dyes were diluted into aqueous solution fresh on the day of the assay or within master mixes stored at -20°C . We routinely keep our dyes protected from light as a general precaution against unwanted photochemical reactions.

SARS-CoV-2 RT-LAMP reaction optimization

We screened LAMP primers for SARS-CoV-2 detection from prior work^{8–10} and found the best performance using

those of D. Wang, which were designed to detect the viral N gene: D.Wang N-gene Forward Loop Primer, D.Wang N-gene Backward Inner Primer, D.Wang N-gene Forward Outer Primer, D.Wang N-gene Backward Outer Primer, D.Wang N-gene Forward Loop Primer and D.Wang N-gene Backward Loop Primer. These and other oligonucleotides were purchased from Integrated DNA Technologies with standard desalting and are listed in **Table 1**.

RT-LAMP reactions contained 8 mM MgSO_4 , 30 mM KCl, 1% Tween 20, 1.6 μM or 0.8 μM FIB/BIP primers as referenced, 0.2 μM F3/B3 primers, 0.4 μM FL/BL primers, 1.4 mM each deoxyribonucleotide triphosphate, colorimetric/fluorescent dyes as above, 7 U of WarmStart Reverse Transcriptase [M0380; New England Biolabs (NEB), Ipswich, MA, USA], 8 U of 120,000 U/ml Bst 2.0 polymerase (NEB MO537), 40 U of NxGen RNase Inhibitor (Lucigen 30281) when working with Universal Transport Media (UTM), Viral Transport Media (VTM), or patient samples. MgSO_4 (M65; Thermo Fisher Scientific, Waltham, MA, USA) and KCl (P9333; MilliporeSigma, Burlington, MA, USA) stocks were made using nuclease-free water prior to dilution to working concentrations. The pH was adjusted depending on the sample. **Table 2** defines the appropriate buffer conditions for each type of reaction. When using VTM or water with

TABLE 1

Oligonucleotides used in this study

Name	Purpose	Sequence
DW N FIP	LAMP	5'-tcccctactgctgctggagtttccggcagtcagccttc-3'
DW N BIP	LAMP	5'-tctgtagaatggctggcaatttttctctcaagctggttca-3'
DW N F3	LAMP	5'-gccaaaaggcttctacgca-3'
DW N B3	LAMP	5'-ttggcctgtgtgttgg-3'
DW N LF	LAMP	5'-cgactacgtgatgaggaacga-3'
DW N LB	LAMP	5'-gcggtgatgctgctct-3'
HCoV-229E-N-T7-fwd	IVT	5'-gaaattaatacactcactatagatggctacagtcacaaatgggctgat-3'
HCoV-229E-N-full-rev	IVT	5'-ttagttgacttcatcaattatgtcagt-3'
229E-N-fwd	qPCR	5'-cgaaagaattcagaaccagag-3'
229E-N-rev	qPCR	5'-gggagtcaggttctcaaca-3'
229E-N-Probe	qPCR	5'-6-FAM-ccacactcaatcaaaagctcccaaat-IBFQ-3'
SARS-T7-Fwd	IVT	5'-gaaattaatacactcactatagatgtctgataatggaccccaaac-3'
SARS-Rev2	IVT	5'-gaccacgtctcccaaatgctg-3'
MERS-T7-Fwd	IVT	5'-gaaattaatacactcactatagatggcatcccctgctgcacctcg-3'
MERS-Rev2	IVT	5'-ggcccgcgaagacaaaagctg-3'
RPP30(13) FIP	LAMP	5'- agtttccatggagaagcgttttctgttggctctctgaa-3'
RPP30(13) BIP	LAMP	5'-tatctctacagtgaagaacctcggttttctggaagctggaagac-3'
RPP30(13) F3	LAMP	5'-tgactggcaaatctagg-3'
RPP30(13) B3	LAMP	5'-actgggcatctttcag-3'
RPP30(13) LF	LAMP	5'-gttggtagaccgc-3'
RPP30(13) LB	LAMP	5'-ccatcagaaggagatgaagatt-3'
18S FIP	LAMP	5'-tggcctcagttccgaaacaaatttctggataccgcagctagg-3'
18S BIP	LAMP	5'-ggcattcgtatggcgccttttggcaaatgcttctgctg-3'
18S F3	LAMP	5'-gttcaagcaggcccgag-3'
18S B3	LAMP	5'-cctccgacttctgttga-3'
18S LF	LAMP	5'-agaaccggtctctattccattatt-3'
18S LB	LAMP	5'-attctggaccgcgcaag-3'
RPP30 T7 Fwd	IVT	5'-gaaattaatacactcactatagggctcaggacttcagcatgg-3'
RPP30 Rev	IVT	5'- ttaaaacaagaggaactaaagtcactt-3'
RPP30q Fwd	qPCR	5'-agattggacctgcgagcg-3'
RPP30q Rev	qPCR	5'-ttctgacctgaaggctctgcgcg-3'
Rpp30 probe	qPCR	5'-FAM-gagcggctgtctccacaagt-BHQ-1-3'

IVT, In Vitro Transcription

LAMPshade Violet, reactions were run using 1 mM Tris-HCl (pH 9.5) and 0.5 mM KOH. To account for HEPES buffer, reactions with UTM were run using 2 mM Tris-HCl (pH 9.5) and 1 mM KOH. Test samples were typically added at 2 μ l, although 4 μ l can be tolerated. The final reaction volume was 25 μ l.

TABLE 2

Variable buffer composition optimizations for VTM

Medium	Indicator	mM Tris pH 8.5	mM Tris pH 9.5	mM KOH
UTM	LSM	—	2	1
UTM	LSV	—	2	1
VTM	LSM	1	—	1
VTM	LSV	—	1	0.5
Saline	LSM	2	—	1
Saline	LSV	—	1	0.5

The DW N primer reactions were run at 60°C with positive/negative readouts after 45 min. The pH-dependent color change could be quantitatively defined by absorbance or fluorescence. However, to establish a low-cost and technically minimal procedure, we chose to rely on visual inspection and qualitatively define a negative reaction as one that retained the negative control color intensity and a positive reaction as one which retained no color when viewed against a white background. Reactions were heated using either an Applied Biosystems 2720 or GeneAmp 9700 thermocycler. Use of a water bath with mineral oil sample overlay yielded equivalent performance. Reactions were typically monitored and photographed at 15-min intervals to document reaction progress. Preliminary assay optimization was performed with quantified N gene plasmid DNA (10006625; Integrated DNA Technologies) and *in vitro* transcribed RNA. However, we sought to utilize a standard that would more closely mimic clinical tests

and found more consistent performance using heat-inactivated SARS-CoV-2 virus (HI-SARS-CoV-2) (VR-1986HK; American Type Culture Collection (ATCC), Manassas, VA, USA, and NR-52286; BEI Resources). Using half of the concentration of WarmStart RT (NEB) was well tolerated; however, data presented in this manuscript consistently used 7 U per reaction. Substituting Maloney Murine Leukemia Virus-RT was not successful, but Superscript IV RT and Maxima H minus RT could feasibly be used in lieu of WarmStart RT, although this required further optimization. Substitution of Bst 3.0 (M0374S; NEB) without WarmStart RT for Bst 2.0 was unsuccessful. Addition of 40 mM guanidine hydrochloride¹¹ decreased the reaction time but also shortened the time interval between the assay endpoint and the nonspecific color conversion of the no-template controls.

Virus sample processing and yields

Human coronavirus 229E (HCoV-229E) was obtained from ATCC (VR-740) and propagated in MRC-5 cells cultured in Eagle's minimum essential medium supplemented with 10% v/v fetal bovine serum and 1× antibiotic-antimycotic solution (Thermo Fisher Scientific) at 37°C, 5% CO₂ incubator. Upon the viral infection, cells were incubated at 35°C, 5% CO₂ incubator for 2 h. The medium was replaced with Eagle's minimum essential medium with 2% fetal bovine serum and 1× antibiotic-antimycotic solution and further incubated at 35°C for 48–72 h until cytopathic effect was exhibited. On the day of harvest, supernatant from the infected MRC-5 cells was collected. Dilute viral supernatants were used directly in spike experiments. HCoV-229E qRT-PCR standard for the viral N gene was prepared from viral genomic RNA extracted from the original virus stock (ATCC) using QiAmp viral RNA Mini Kit. The cDNA was synthesized using PrimeScript first-strand cDNA synthesis kit (Takara, Kyoto, Japan) followed by PCR with the primers HCoV-229E-N-T7-fwd and HCoV-229E-N-full-rev (Table 1). PCR was performed using GoTaq Green Mix (M7122; Promega, Madison, WI, USA) according to the manufacturer's instructions. The *in vitro* transcribed RNA was prepared using the T7 RiboMAX Express System (1280; Promega).

For detection of HCoV-229E, SuperScript III Platinum One-Step qRT-PCR kit (11732088; Thermo Fisher Scientific) was used. Additional MgSO₄ was added to bring the final [Mg²⁺] = 3.8 mM. The reaction mixture was prepared to 23 µl, and 2 µl of samples was added for a final reaction volume of 25 µl. qRT-PCR was performed using the Roche LC480 with the following condition: reverse transcription at 55°C for 20 min, denaturation at 95°C for 3 min, amplification of 50 cycles at 95°C for 15 s

followed by 58°C for 30 s, and cooling at 40°C for 30 s. qRT-PCR primers for the N gene were 229E-N-fwd, 229E-N-rev, and 229E-N-Probe (Table 1).¹²

In silico analysis of LAMP assay primers

To determine the organism exclusivity and specificity of the DW LAMP primer set, we downloaded 44,899 genomes from the National Center for Biotechnology Information (NCBI) Virus SARS-CoV-2 data hub (<https://www.ncbi.nlm.nih.gov/labs/virus/vssi/#/>) on December 9, 2020. We selected 43,849 sequences that had an identifiable N gene using the search string ATGTCTGATAATGGACCCCA from RefSeq NC_045512.2 for the SARS-CoV-2 N gene. The N gene sequences were extracted by selecting up to 1260 bases downstream from the start of the search string using a custom python script. This subset was filtered to remove sequences containing homopolymers of 3 or more undetermined ("N") bases, leaving 41,889 high-quality N gene sequences. This list was then filtered to remove sequences that were <750 bases. This requirement ensured the selected N genes would include the DW LAMP primer set. The remaining 41,858 sequences were then mapped to the the N gene RefSeq using Geneious Prime software (Biomatters, Ltd., 2020 version), and the multiple alignment was exported as a fasta alignment file. Per-base mismatches were calculated by counting the number of exact matches at each position and subtracting from 41,858 using Linux command line utilities. Sequence homology between the DW LAMP primer set and SARS-CoV ZJ01 was determined using the Map Primers function in Geneious Prime, with NCBI accession AY297028 as the reference and DW LAMP primers truncated to remove the loop regions as the query. The analysis was repeated for Middle East Respiratory-CoV using NC_028752.1 as the reference.

LAMP assay specificity and exclusivity

Plasmid DNA templates were acquired from Integrated DNA Technologies for MERS-CoV and SARS-CoV (10006623 and 10006624). For SARS-CoV, MERS-CoV2 RNA standards, PCR reactions were performed as described above using a T7 promoter containing primer sets targeting the N gene of each control plasmid using primers SARS-T7-Fwd, SARS-Rev2, MERS-T7-Fwd, and MERS-Rev2 (Table 1). The PCR amplicons were confirmed by agarose electrophoresis and purified with DNA clean-up columns (Zymo Research). RNA was synthesized from clean PCR products using the T7 RiboMAX Express System as above. The *in vitro* transcribed RNAs were purified with Monarch RNA Cleanup Kit (T2040; NEB), divided into aliquots, and stored at −80°C until used.

RNA was quantified using a Nanodrop spectrophotometer using appropriate extinction coefficients. Natrol Respiratory Panel 2 controls were purchased from Zeptomatrix (NATRPC2-BIO). RNA was extracted from these mixed-organism panels using the QiAmp viral RNA Mini Kit (52904; Qiagen, Germantown, MD, USA). qRT-PCR for the HCoV-229E N gene was performed to confirm the success of the RNA preparation from these panels, which yielded 2030 HCoV-229E copies per μl .

Nonpatient test samples and transport media

Normal human saliva was purchased from BioIVT from 5 males and 5 females, with ages ranging from 27 to 42 y old, and a mix of races including Asian, Black, Caucasian, and Hispanic. Sputum was purchased from Discovery Life Sciences (BBL0000-AI900368151011420DD). Sputum remnant samples had been collected as potential tuberculosis diagnoses but were deemed negative. Clean VTM was prepared as described by the Centers for Disease Control and Prevention (CDC) (<https://www.cdc.gov/coronavirus/2019-ncov/downloads/Viral-Transport-Medium.pdf>).

UTM is a proprietary formulation (Copan) and was acquired and donated by Carolyn Walsh, MD. HI-SARS-CoV-2 was purchased from ATCC or BEI (VR-1986HK, ATCC, and NR-52286, BEI).

Patient sample collection and testing

SARS-CoV-2–negative and –positive NP swab samples were obtained by agreement from Johns Hopkins University. Samples had originally been collected in UTM and tested by either the NeuMoDx SARS-CoV-2 or the Real-Star(R) SARS-CoV-2 RT-PCR assays.^{13,14} An aliquot of 250 μl was frozen at -80°C after testing. In total, 30 SARS-CoV-2–positive samples (Ct values ranging from 14.13 to 41.35) and 10 SARS-CoV-2–negative samples were included in this study.

RNAse P subunit 30 (RPP30) and 18S rRNA sample integrity control LAMP. LAMP primers for the human RPP30 RNA were designed using the online software Primer Explorer v5 (available at <http://primerexplorer.jp/e/>). The RPP30 primers are RNA specific, as they span at least one genomic intron. RPP30(13) FIP, RPP30(13) BIP, RPP30(13) F3, RPP30(13) B3, RPP30(13) LF, and RPP30(13) LB are listed in Table 1. 18S rRNA primers were adapted from Lamb *et al.*¹⁵ 18S FIP, 18S BIP, 18S F3, 18S B3, 18S LF, and 18S LB are also shown in Table 1. RT-LAMP assays were done using unextracted dilutions of human HEK293 cells. Cells were counted, resuspended in water, and stored at -80°C prior to direct use in LAMP reactions. RPP30 RNA amounts in HEK293 were quantified using qRT-PCR against a reference control using

purified cellular RNA. For the RPP30 RNA standard, cellular RNA from HEK293T cells was extracted, cDNA was synthesized, PCR was performed with T7 promoter containing primer sets, and the *in vitro* transcribed RNA was prepared as described above. Primers for the *in vitro* transcription amplicon are RPP30 T7 Fwd and RPP30 Rev. qRT-PCR primers for the RPP30 gene are RPP30q Fwd, RPP30q Rev, and Rpp30 probe (Table 1). Each HEK293 cell was determined to contain on average 9.5 copies of detectable RPP30 RNA.

RESULTS

Use of novel pH indicator LAMPshade dyes

We screened a panel of possible pH-sensitive dyes based on carbofluorescein and Si-fluorescein for their utility in LAMP assays. We identified 2 compounds that showed optimal contrast and performance: carbofluorescein (LAMPshade Magenta) and 4,5,6,7-tetrafluoro-Si-fluorescein (LAMPshade Violet; Fig. 1B, C).^{6,7} Examination of the pH titration of these dyes reveal they both exhibit optimal pK_a values ($pK_a = 7.08$ and 7.48) for LAMP reactions performed under low buffering capacity, which are initiated at $\sim\text{pH } 8.5$ and are complete at $\sim\text{pH } 6.0$.⁵ In addition, both LAMPshade dyes exhibit a cooperative transition between a highly colored dianionic species and a colorless lactone form, resulting in a steep colorimetric/fluorometric pH-dependent transition, reflected in their Hill coefficients being greater than 1 (Fig 1C). We compared the pH sensitivity of the LAMPshade dyes to the common pH indicator Phenol Red, which has been used for visual detection of LAMP reactions and is a component in commercial assay kits (Fig. 2A). Aqueous solutions of the LAMPshade dyes are highly colored at pH values above their pK_a but are colorless at pH values below their pK_a with a relatively steep transition. In contrast, Phenol Red changes from red to yellow as pH decreases. The Phenol Red ratiometric readout and shallower transition can lead to ambiguous determinations, especially using visual readout with colorblind individuals. We then compared these dyes in LAMP assays (Fig. 2B) using weakly buffered conditions. Consistent with the pH titration, the LAMPshade dyes offer a greater contrast because of their binary response and steeper color transition. In addition to yielding colorimetric readouts by eye, the LAMPshade dyes can be visualized using fluorescence excitation with a handheld UV light (Fig. 2C) or measured in a fluorescence plate reader, a quantitative PCR instrument, or other spectrometer or fluorometer instrument. Here, we chose to focus on visual colorimetric readout to minimize technical barriers.

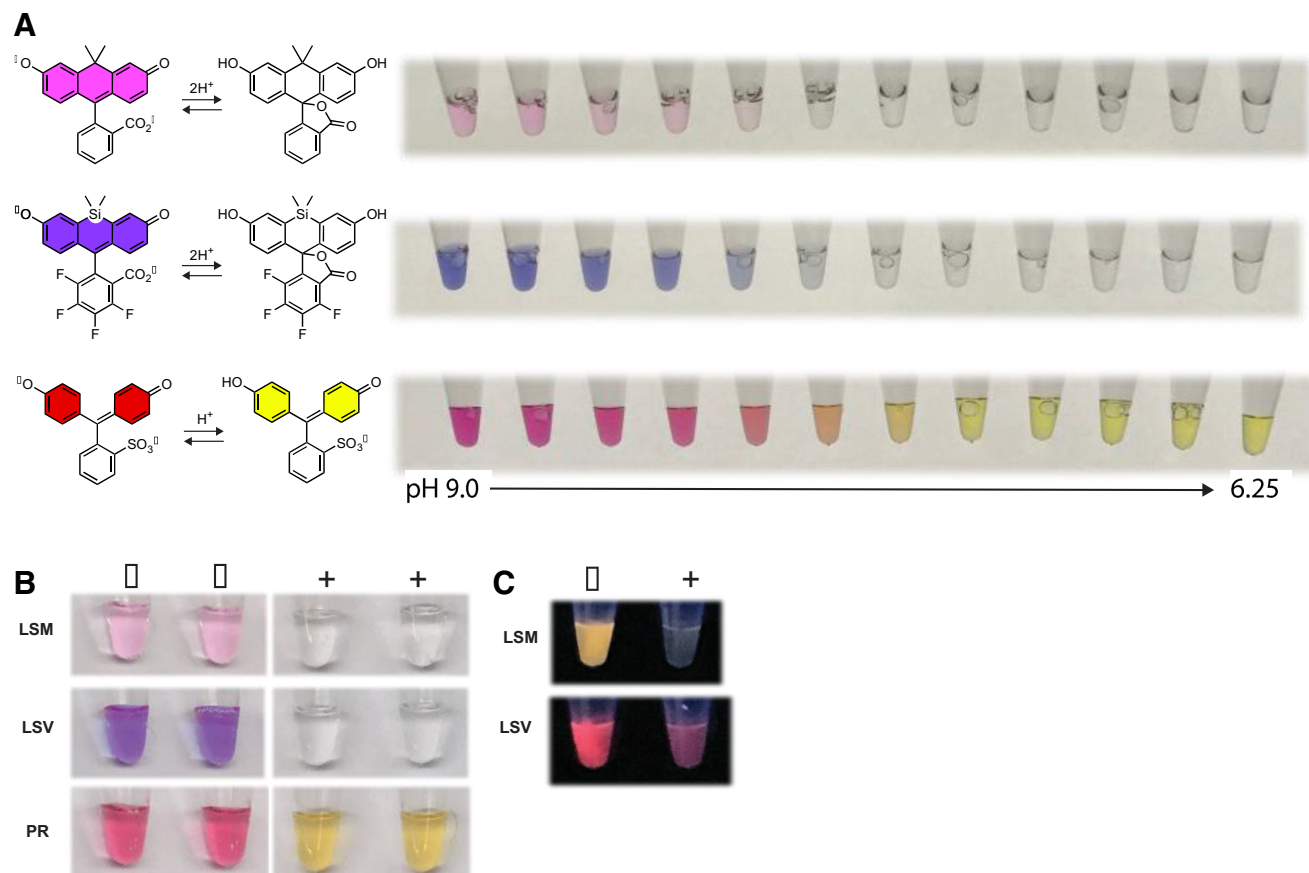


FIGURE 2

Colorimetric dye pH response and LAMP readouts with various pH indicators. A) Images of solutions of LAMPshade Magenta, LAMPshade Violet, and Phenol Red at varying pH values ranging from pH 9.0 to 6.25 in 0.25-U increments, left to right. B) Images of negative (-) and positive (+) jLAMP reactions under normal light. C) Images under handheld UV (365 nm) light using LAMPshade Magenta and Violet.

LAMP primers and reaction optimization

Having established the utility of the LAMPshade dyes in the LAMP assay, we focused on optimizing the reaction for SARS-CoV-2 detection. We envisioned jLAMP assay workflow as displayed in **Fig. 3A**, where heat-treated swab media or saliva is directly added to the jLAMP master mix, heated at 60°C, and read out visually. First, we screened several sets of LAMP primers^{8–10} to achieve optimum performance and found that those designed by D. Wang¹⁰ yielded the best sensitivity. We also designed primers specific for the human RPP30 and 18S rRNA genes to be used to test sample integrity. Second, we considered the buffer composition, as commercial assay kits use proprietary formulations. Buffer choice is influenced by many factors, including the transport media used for the sample and the specific pK_a of the LAMPshade dye. After numerous buffer iterations, we found 1–2 mM Tris-HCl buffer as an acceptable starting concentration; higher concentrations

(>3 mM) resulted in reactions that were slower to change the indicator color and prolonged the assay. The pH tuning of these buffers for various VTM is shown in Table 2. Finally, we optimized the assay duration, as LAMP primers can form non-template-mediated self-constructions given enough time, starting the exponential amplification. We defined the endpoint of the assay as the time at least 30 min prior to the typical conversion of nontemplate control sample; endpoints ranged from 30 to 60 min depending on the primer set.

Effect of virus sample handling and processing in direct qRT-PCR

RNA purification from patient samples is commonly employed in qRT-PCR and other nucleic acid assays. To reduce cost and complexity, we sought to define conditions in which the jLAMP assay could function without RNA extraction using direct addition of sample to the reaction.

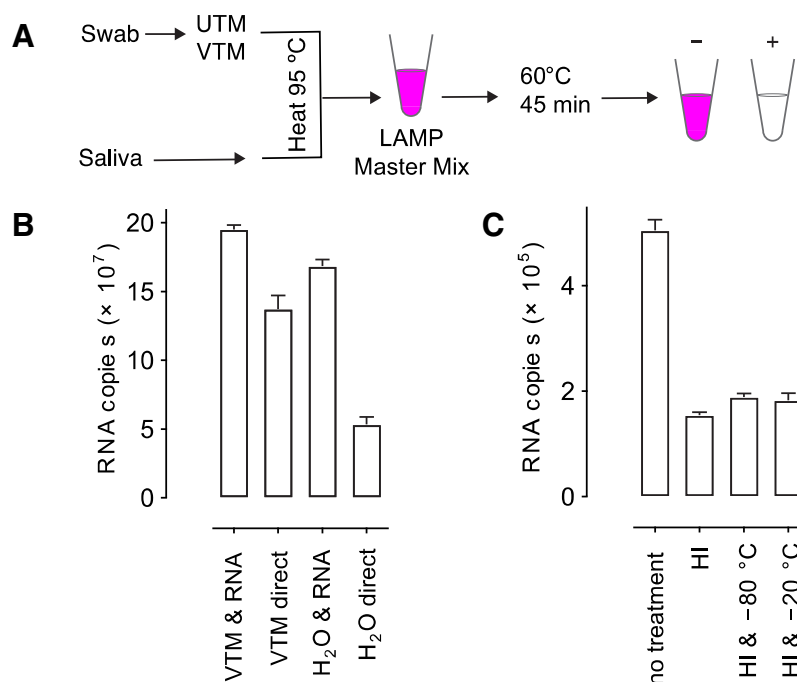


FIGURE 3

jLAMP assay optimization. A) Workflow of jLAMP assay. B) Comparison of HCoV-229E viral RNA detected after RNA purification or directly from samples in either VTM or H₂O. Data represent averages of 4 replicates showing standard deviation bars. C) Effects of heat and freeze-thaw treatments on RNA recovery in direct qRT-PCR sample assays. Heat-inactivated (HI) samples were heated to 65°C for 30 min. Data represent averages of triplicate samples with standard deviation bars.

As a proxy for SARS-CoV-2, we used the nonlethal HCoV-229E strain to test for the availability of viral RNA using qRT-PCR under different conditions. The propagated HCoV-229E was diluted and spiked into VTM or deionized water. Samples were either processed by RNA extraction followed by qRT-PCR or directly used in qRT-PCR. Direct assay of HCoV-229E in VTM yielded 70% of the RNA-extracted sample (Fig. 3B). RNA detection from HCoV-229E in water was only 31% of the RNA-extracted control. Additional experiments indicated that serum proteins in VTM are responsible for the increased recoveries relative to water (data not shown). Assuming that HCoV-229E is similar to SARS-CoV-2, we inferred from these data that direct testing of viral samples without RNA extraction was feasible with a 30% loss of sensitivity when using VTM.

In addition to RNA extraction, clinical COVID-19 samples are often heat inactivated to limit viral exposure during handling and then stored frozen. We tested the effects of a heat inactivation and a single freeze/thaw cycle. HCoV-229E was spiked into VTM and divided into 4 tubes. Each tube was further exposed to heat inactivation at 65°C for 30 min and different storage conditions (Fig. 3C). Heat inactivation decreased the available RNA to about 33% of the control but additional freeze/thaw treatment did not further decrease the recovery. Thus, employing both freeze/thaw and viral heat inactivation in the testing workflow is reasonable but does further affect sensitivity.

Limits of detection and false positives in viral sample media

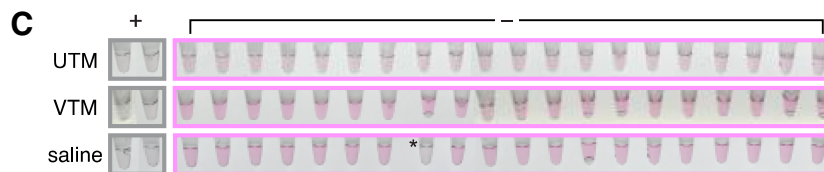
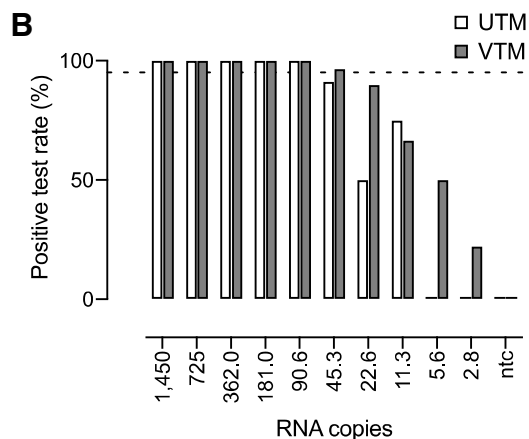
Although our RT-LAMP assay was initially developed with synthetic RNA templates, we found that the most useful biomimetic was to test various media that had been spiked with known amounts of HI-SARS-CoV-2. **Figure 4A** displays data compiled from multiple independent experiments to determine assay sensitivity in various CDC/World Health Organization–approved nasal swab media used in sample collection from patients with COVID-19. This includes UTM, VTM, and normal saline (0.9% w/w). Clean sample medium was spiked with various dilutions of HI-SARS-CoV-2 virus (ATCC) and tested directly, without RNA purification or processing. The 95% limit of detection (LoD) is defined in the Food and Drug Administration’s emergency use authorization guidelines as the RNA copy number that is detected at 95% frequency or better from at least 20 samples. UTM is somewhat inhibitory relative to VTM and saline, with 95% LoD values of 90.6, 45.3, and 22.6 RNA copies, respectively. The lowest LoDs are 11.3, 2.8, and 2.8, respectively. UTM shows a more defined detection cutoff below 11.3 RNA copies per reaction (Fig. 4B).

LAMP reactions can yield false-positive results because there is a small but significant probability for some combination of the 6 primers to self-assemble into nonspecific, primer-only DNA amplifications. The frequency of these events increases with time. We surveyed different reaction durations to determine reaction conditions that balance

A	Transport Media	95% LoD RNA copies	Lower Limit RNA copies
	UTM	90.6	11.3
	VTM	45.3	2.8
	Saline	22.6	2.8

FIGURE 4

Sensitivity and specificity of jLAMP. *A*) Limits of detection of jLAMP in various VTM spiked with HI-SARS-CoV-2. Data were compiled from multiple independent experiments. *B*) jLAMP sensitivity in UTM and VTM at low viral copy numbers. *C*) False-positive (no viral RNA) frequency in different swab sample transport media: VTM, UTM, or saline. Positive controls (+) contained HI-SARS-CoV-2 at ~260 copies. The single positive in saline is marked with an asterisk. One sample out of 60 yields a 1.66% false-positive percentage. Positive reactions were determined by lack of color detection and comparison to controls by visual inspection against a white background.



high sensitivity with low false positives for this endpoint assay, arriving at 45 min of incubation. To validate this choice using the DW primers, we tested the frequency of nontemplate constructions using clean virus sample buffers. In total, 20 replicates for each of the 3 samples buffers were run without template (Fig. 4C). Only 1 tube of the 60 replicates turned clear, representing a false-positive rate of 1.66%. As with all LAMP-based assays, increasing incubation time beyond this endpoint is expected to increase sensitivity at the cost of greater false positivity.

LAMP sensitivity in spiked negative NP swab samples

We obtained clinical NP swab samples in UTM, which were identified as negative for SARS-CoV-2 RNA by RT-PCR. A subset of these samples ($n = 13$) were spiked with serial dilutions of HI-SARS-CoV-2 virus and assayed to determine the degree of inhibition that might be contributed by native RNases, mucus, and other substances from nasal secretions transferred into the swab media. **Figure 5A** shows the percent detection at each of the SARS-CoV-2 dilution values. Although in this specific experiment we did not achieve the 95% LoD of 90.6 RNA copies, there was minimal inhibition relative to clean UTM (Fig. 4B), and we could detect lower amounts of RNA with modest reproducibility,

detecting 5.6 RNA copies and 2.8 RNA copies in 38.5% and 30.8% of the samples, respectively.

Preliminary validation of LAMP using direct saliva samples and sputum

To assess the feasibility of performing the LAMP assay directly on saliva samples, we ran several experiments using normal saliva spiked with HI-SARS-CoV-2. Untreated saliva was inhibitory and showed a large variation between samples. During initial trials using proteases to degrade RNases, we found that treating samples at 95°C for 10 min needed for protease inactivation achieved the same results with or without protease. Fig. 5B shows that after heat treating saliva from 8 individuals and a subsequent challenge with 23 viral copies, all samples supported LAMP detection, albeit at varying detection efficiencies. Sputum samples were also tested after treatment with DTT and diluted prior to spiking with HI-SARS-CoV-2 virus. The LAMP assay failed to detect viral RNA in these samples (data not shown).

LAMP performance with direct assay of NP swab samples of patients with COVID-19

We then compared the efficacy of the LAMP assay with a qRT-PCR using clinical samples. We used COVID-19

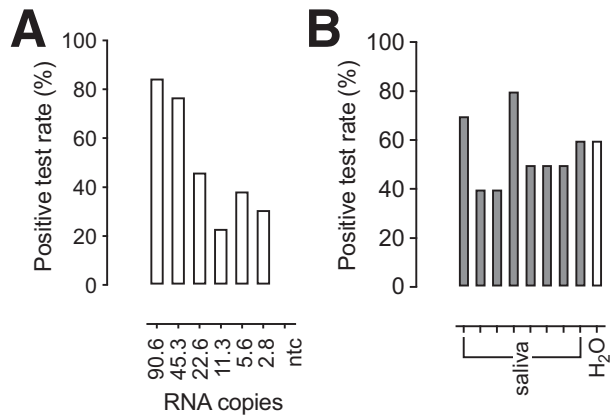


FIGURE 5

jLAMP assay optimization. A) jLAMP sensitivity in COVID-19–negative NP swab samples. In total, 13 COVID-19 negative samples were spiked with serially diluted heat-inactivated SARS-CoV-2. Percent positive samples are plotted against the corresponding RNA copy values; LAMP reactions were performed with LAMPshade Magenta. Each bar represents the percent positivity rate for 13 samples in duplicate. B) Saliva sample testing for LAMP performance. In total, 8 normal saliva samples were spiked with 23 copies of heat-inactivated SARS-CoV-2 ($n = 10$). Percent positive for each saliva sample is displayed relative to a water control.

samples from patients that were designated as positive using a sensitive 2-gene qRT-PCR assay (Altona).¹³ In this initial diagnostic PCR assay, a portion of the swab sample was subjected to RNA extraction protocol, concentrated 10-fold after RNA extraction, and a 10- μ l RNA volume was added to the qRT-PCR master mix. In contrast, the jLAMP assay uses 2 μ l of direct sample, circumventing the RNA extraction and concentration steps. We expected lower sensitivity relative to the qRT-PCR, as the jLAMP assay uses 50 \times less starting material than the qRT-PCR assay, with further loss of sensitivity due to the use of UTM (Fig. 4B) and other factors mentioned above. **Figure 6** displays jLAMP test results from each of the samples from patients positive for COVID-19 against the corresponding C_t values from a second qRT-PCR assay using the CDC N gene primer set. The jLAMP successfully detected RNA in 23 of the 30 original positive samples. Sensitivity tapered off below 157 RNA copies, while still detecting about 17.4 copies ($C_t = 36.2$); the assay failed to detect genome numbers below 10 copies in these patient samples. We note that 4 of LAMP-negative samples were also negative using CDC N gene qRT-PCR, likely because of the lack of RNA concentration after purification, the lowered amount of test volume, or the heat inactivation of these samples. We also tested 30 negative COVID-19 patient samples; all but one tested negative in the LAMP reactions. Interestingly, this solitary sample was retested using qRT-PCR and found to be a false negative ($C_t = 37.2$; data not shown).

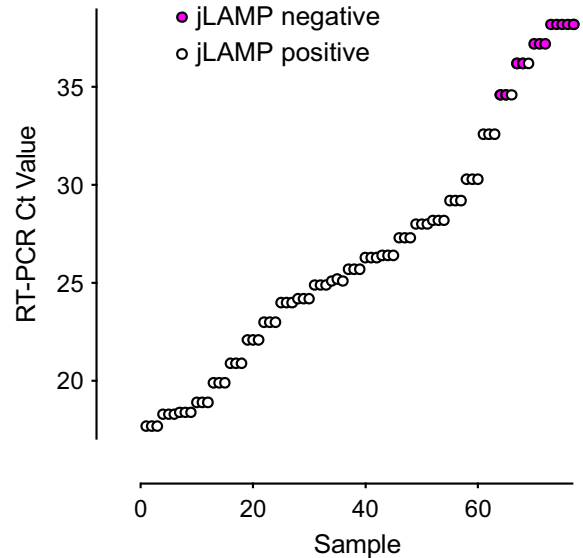


FIGURE 6

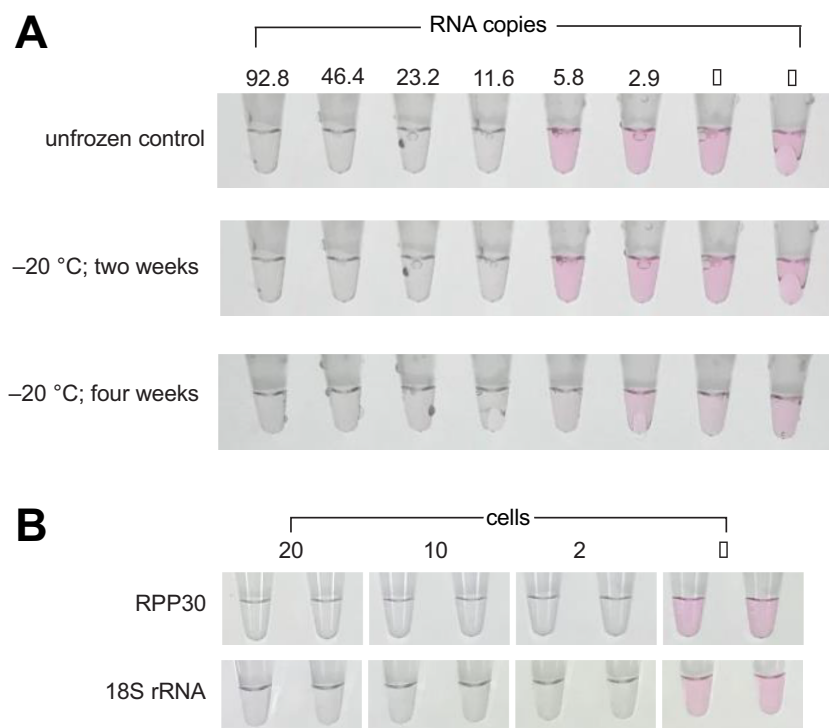
COVID-19 patient nasal swab quantification and jLAMP test results. SARS-CoV-2–positive NP swabs in UTM were LAMP tested ($n = 30$). Each sample was assayed in triplicate, and all data points are shown in the plot. Each data point is assigned a sample number (x axis) ranked by C_t value. qRT-PCR C_t values obtained from the CDC N gene primer set are reported based on assays after heat inactivation. LAMP positive samples are represented by clear circles, and negative samples are displayed as red.

LAMP primer specificity

We conducted an *in silico* analysis to determine the organism exclusivity and specificity of the DW LAMP primer set. We aligned the primer sequences to 41,858 high-quality genomes from the NCBI Virus SARS-CoV-2 data hub that contained the LAMP assay primer region in the N gene from RefSeq NC_045512.2 (see Materials and Methods). The sequence identity for all 6 LAMP primers in this alignment was 99.8% or greater, and the per-base mismatches for the last 5 nucleotides of each primer were quantified. The greatest frequency of mismatches is within the FIP primer at the -4 position, which should be well tolerated. It is therefore likely that this primer set will detect all sequence variants of SARS-CoV-2 (as of December 9, 2020), although some variants may amplify with less efficiency. However, all 6 LAMP primers also have partial or complete sequence identity with the SARS coronavirus ZJ01. This implies that patients with SARS-CoV from the original pandemic in 2003 could test positive with this assay. Only 1 primer (Wang LB) had partial sequence identity with MERS-CoV, which is insufficient to generate LAMP products. We confirmed the *in silico* analysis using the LAMP primer set using RNA from SARS-CoV and MERS-CoV. Finally, to control for false positives stemming

FIGURE 7

LAMP master mix storage stability and integrity controls. A) Tube labels with 2-fold serial dilutions of SARS-CoV-2 from 92.8 to 2.9 copies: top, unfrozen control; middle, -20°C storage for 2 wk; bottom, -20°C storage for 4 wk. B) LAMP assays for RPP30 and 18S rRNA as sample integrity controls. RPP30 (RNaseP subunit) and 18S rRNA LAMP primers were tested on HEK293 mammalian cells at 20, 10, and 2 cells per tube in duplicate.



from other organisms expected to be present within patient swabs, we used a respiratory control panel of bacteria and viruses obtained from Zepetrix (data not shown). Controls included adenovirus type 1, adenovirus type 3, adenovirus type 31, *C. pneumoniae*, influenza A H1N1 pandemic, influenza H3N2, metapneumovirus type 8, *Mycoplasma pneumoniae*, parainfluenza type 1, parainfluenza type 4, and rhinovirus type 1A, *Bordetella parapertussis*, *Bordetella pertussis*, coronavirus HKU-1, coronavirus NL63, coronavirus OC43, influenza A H1N1, influenza B, parainfluenza type 2, parainfluenza type 3, and Respiratory syncytial virus type A. The LAMP assay was negative with these control panels, yielding no cross-specificity from these pathogens.

LAMP master mix stability

To simplify deployment logistics, we sought to create a stable master mix of our LAMP components to which only test sample is applied. The master mix could then be prepared and frozen for later use at a near-patient testing site. We screened a panel of 11 cryoprotectants, testing both assay interference and cryoprotective ability. The panel included various disaccharides (sucrose, maltose, trehalose at 12.5–50%), glycerol (12.5–50%), polyethylene glycol 400 (12.5–50%), polyethylene glycol 200 (12.5–50%), proline (0.5–2 M), ethylene glycol (12.5–50%), lithium sulfate (0.25–1 M), sodium malonate

(0.85–1.7 M), and 1-methyl 2,4 pentanediol (12.5–50%). Surprisingly, we found the least assay interference and best stability in formulations that had none of these cryoprotectants. The original master mix is stable for at least 4 wk when stored at -20°C without loss of sensitivity (Fig. 7A).

LAMP with sample integrity control primers for RNaseP (RPP30) and 18S rRNA

To determine RNA presence and integrity in COVID-19 patient samples, an appropriate control assay should be applied to all negative sample reads. The human RPP30 and 18S rRNA genes are highly expressed and have been used as sequence targets for sample integrity tests. We tested sets of LAMP primers for both RPP30 and 18S rRNA and validated them using human HEK293 cells as a biomimic for patient cells transferred from nasal swabs. Figure 7B shows that both of these primer sets can detect as low as 2 HEK293 cells per assay. We quantified the RNA transcript level in HEK293 cells using qRT-PCR and determined that 2 cells contain approximately 19 copies of RPP30 RNA.

DISCUSSION

Robust, accurate, and inexpensive COVID-19 diagnostic tests are a cornerstone of pandemic management strategies. RT-LAMP is a simple viable alternative to the standard

qRT-PCR and can fill the need for a complementary COVID-19 test in near-patient venues without the need for expensive instruments and highly trained personnel. In addition, RT-LAMP can be less expensive and does not compete with the qRT-PCR reagent supply chain. We describe here the jLAMP assay, which uses novel colorimetric pH indicators, LAMPshade Violet and LAMPshade Magenta. The jLAMP assay using these dyes can be used without RNA extraction and is sensitive, specific, robust, simple, and inexpensive.

The use of pH indicators in LAMP assays was pioneered by Tanner and colleagues at New England Biolabs, who leveraged the large change in pH that occurs during the LAMP reaction from pH 8.5 to pH 6–6.5.⁵ Although Phenol Red is the most popular colorimetric LAMP indicator, it has several disadvantages. First, Phenol Red has relatively high $pK_a = 8.0$, which is close to the starting pH of the LAMP assay. This makes the indicator sensitive to acidic samples even in the absence of DNA amplification. Phenol Red undergoes a gradual color transition from pink above pH 8.2 to yellow below pH 6.8. This decrease in one color (pink) and increase in the other color (yellow) can lead to ambiguous color determination and, therefore, interpretation of test results. Finally, the Phenol Red exhibits poor fluorescence properties, limiting use to colorimetric assays. In contrast, the LAMPshade dyes exhibit lower pK_a values, show a colored-to-colorless transition, and can be used as either colorimetric or fluorescence indicators (Fig. 1C), depending on the availability of instrumentation or desire to eliminate qualitative visual readouts. Other colorimetric dyes have also been used as LAMP readouts, including leuco Crystal Violet,¹⁶ Calcein,¹⁷ and Hydroxynaphthol Blue,¹⁸ which detect double-stranded DNA or Mg^{2+} . Nevertheless, these dyes yield results that are arguably more ambiguous than the pH-based assays using Phenol Red or the LAMPshade dyes.

A critical step in simplifying COVID-19 testing is avoiding the purification of RNA as the first step. This eliminates time, cost, and supply-chain bottlenecks for RNA purification reagents and kits. We quantified the loss of detection sensitivity in direct sample assays on treated samples using HCoV-229E as a proxy for SARS-CoV-2. The direct assay showed 70% sensitivity relative to the purified RNA, likely reflecting some inaccessibility of the encapsulated viral RNA in direct sampling using qRT-PCR. RNA purification also serves to inactivate the virus, allowing for increased laboratory safety. We tested a 30-min, 65°C heat inactivation and achieved 33% sensitivity relative to nonheated samples. Although this heat treatment is sufficient to inactivate SARS-CoV-2,¹⁹ it may allow degradation of RNA and loss of sensitivity. Heat treatment at 98°C has been shown to improve sensitivity

in LAMP assays.²⁰ An additional caveat here is that HCoV-229E may not behave as SARS-CoV-2 in direct assays, as others have reported 97% sensitivity with a similar heat treatment.¹⁴ Regardless, our data are consistent with others that direct assays and heat inactivation both support successful RT-LAMP assays, with less sensitivity relative to qRT-PCR using purified viral RNA. We consider this loss of sensitivity a reasonable trade-off in circumventing the disadvantages of RNA purification as a first step. Direct SARS-CoV-2 LAMP assays have been previously tested with varying degrees of success.^{20–24}

The jLAMP assay sensitivity is excellent, with 95% LoD of 22.6 copies per assay (11.3 copies/ μ l) and a lower limit of about 3 copies per assay (1.5 copies/ μ l) in normal saline (Fig. 4A). This analytical sensitivity matches the CDC's 2019-nCoV Real-Time RT-PCR Diagnostic Panel with an LoD of 10 copies/ μ l²⁵ (<https://www.fda.gov/media/134922/download>). Vogels and colleagues²⁶ surveyed the performance of multiple qRT-PCR SARS-CoV-2 primer sets used in testing worldwide and determined that the best primers detected 1 copy/ μ l at 25% frequency and 10 copies/ μ l at 25–50% frequency. Although their assay conditions were less than optimal, the jLAMP assay described here performed similarly at these very low copy numbers (Fig. 5A).

We note that the LoD values are analytical sensitivity measurements and not a measure of clinical performance. In clinical samples, the jLAMP assay had a working sensitivity of about 10 copies/ μ l, which again is comparable to other routinely used clinical diagnostic COVID-19 tests. This level of sensitivity should be adequate if used in a high-frequency surveillance testing regimen, for which absolute sensitivity may be less important than other factors such as testing frequency. Testing for clinical diagnosis may be used to manage patient care, whereas the goal of surveillance testing is to identify and sequester infectious individuals. Larremore *et al.* have argued that for detection of the viral N gene RNA, those people whose samples contain less than 10,000 copies/ μ l are unlikely to have transmissible levels of virus.²⁷ They advocate that a strategy of more frequent testing and fast reporting times largely eliminates the advantages of those tests detecting better than 1000 copies/ μ l. Therefore, jLAMP vastly exceeds this criterion for use in population surveillance with frequent testing.

The specificity and exclusivity are important factors in diagnostic assays as low performance can lead to false-positive readouts. The jLAMP assay with the current primer set is predicted to detect all sequence variants of SARS-CoV-2. Accumulation of mutations in the SARS-CoV-2 population within these primer regions could render these primers dysfunctional. Fortunately, mutational mismatches in the middle or 5' ends of the long, stable

LAMP primers often have little effect on annealing and assay performance, resulting in higher mismatch tolerance than typically obtained with shorter PCR primers. Regardless, monitoring the frequency and distribution of relevant sequence variants should be an ongoing effort to ensure assay integrity. We have also screened a control panel of bacteria and viruses associated with respiratory illness and determined that the jLAMP assay excludes these common organisms. The primers used here do have significant homology to the original SARS-CoV virus, however, and we show that RNA from that virus is detected by the jLAMP assay; the exceedingly low prevalence of SARS-CoV infection minimizes the significance of this assay crosstalk. In addition to the possibility of off-target templates, false positives also arise in LAMP reactions from primer self-constructed amplicons, analogous to primer-dimer formation in PCR. We have determined that the jLAMP yields a false positivity (nonspecific amplification) rate of 1.66% at our defined endpoint (Fig. 4C). Finally, LAMP reactions can generate as much as 10–15 µg of DNA per reaction tube, which is 50 times that typically amplified in a PCR reaction. This leads to higher risk of bench and instrument contamination, which can also increase false positivity. LAMP assay workflows should avoid steps that require multiple additions to the reaction vessel.

Our intention was to create an inexpensive assay that was simple enough to be deployed outside of a complex centralized diagnostic laboratory. To this end, LAMP assays require only a limited number of reagents and a constant heat source. Although developed with standard laboratory pipettors and benchtop thermocyclers, we have also demonstrated equivalent assay performance using an inexpensive water bath (<\$70; Amazon), and disposable glass micropipettes (Drummond). The master mix is stable at –20°C and in the dark for at least 4 wk and can be divided into aliquots into test vessels before field use. Cost and speed are also critical considerations in filling the need for frequent testing strategies. We have calculated the cost of disposable components of jLAMP to be about \$2.88 per sample (\$0.52/plastic, \$0.37/Bst2.0 polymerase, \$1.39/Warmstart Reverse Transcriptase, \$0.08/RNase Inhibitor, \$0.48/deoxyribonucleotide triphosphates, \$0.02/oligonucleotides, \$0.02/dye). This cost would double if the integrity control (RPP30 or 18S rRNA) is to be run in parallel. The assay can be completed in less than 1 hour from sample addition to readout, which is a considerable time savings over most PCR tests.

Although we validated the jLAMP assay using clinical NP swab samples, NP swabbing poses several challenges. These include swab expense and availability, the need for trained personnel, increased exposure to healthcare

personnel, and discomfort to patients. Saliva sampling can circumvent many of these problems and has been shown to perform as well or better than NP swab samples in COVID-19 testing.²⁸ We were unable to obtain COVID-19 patient saliva samples to validate this approach using jLAMP. However, using normal saliva spiked with SARS-CoV-2, we show that the jLAMP assay can support direct testing of saliva (Fig. 5B). The cumulative percent positivity from all 8 saliva samples yields a frequency of 55% at 23 copies per assay. This is somewhat higher than the percent positivity obtained from the same copy presented to normal UTM nasal swabs at 46% (Fig. 4B). This suggests that the assay may perform as well with saliva, if not better than NP swabs in UTM. However, this is a low sample trial, and more work is needed to validate this approach using clinical saliva samples. We have collaborated with M. Rosbash's laboratory (Brandeis University), who has found that some saliva samples are unsuitable for direct LAMP assays using LAMPshade Violet, and further RNA purification is needed to prevent an increase in false positives (data coordinately published).

ACKNOWLEDGMENTS

This work was supported by the Howard Hughes Medical Institute *via* the Janelia Research Campus. H. Mostafa acknowledges research collaboration and contribution with equipment and reagents from Bio-Rad Laboratories, DiaSorin Molecular, collaboration with BD Diagnostics, and honoraria from GenMark. The authors would like to thank Meghan Seltzer, Mike Perham, Anu Bhukel, Kristina Heiberger, and Anastasia Osowski (Janelia), for their logistical help enabling this work. Much of this work was funded as part of the The Tool Translation Team at the Janelia Research Campus. We benefited from discussions with the *ad hoc* COVID-19 Detection Team that quickly formed at Janelia that brought together many discovery scientists from many disciplines to study COVID-19 and join a global network in detecting, understanding, and helping in a moment of crisis; Daryl Carson, Antony Rosen, and Hal Dietz (Johns Hopkins) for their help obtaining clinical samples used to validate our assay; Albert Yu (Brandeis) and Nathan Tanner (New England Biolabs) for useful discussions on LAMP methods; and Chris Mason and the gLAMP consortium and Carolyn Walsh, MD, for clinical insights and reagents.

REFERENCES

1. Notomi T, Okayama H, Masubuchi H, Yonekawa T, Watanabe K, Amino N, et al.. Loop-mediated isothermal amplification of DNA. *Nucleic Acids Res* 2000;28:E63 <https://doi.org/10.1093/nar/28.12.e63>.
2. Wong Y-P, Othman S, Lau Y-L, Radu S, Chee H-Y. Loop-mediated isothermal amplification (LAMP): a versatile technique for detection of micro-organisms. *J Appl Microbiol* 2018;124: 626–643 <https://doi.org/10.1111/jam.13647>.
3. Parida M, Posadas G, Inoue S, Hasebe F, Morita K. Real-time reverse transcription loop-mediated isothermal amplification for rapid detection of West Nile virus. *J Clin Microbiol* 2004;42: 257–263 <https://doi.org/10.1128/JCM.42.1.257-263.2004>.
4. Mori Y, Nagamine K, Tomita N, Notomi T. Detection of loop-mediated isothermal amplification reaction by turbidity derived from magnesium pyrophosphate formation. *Biochem Biophys*

- Res Commun* 2001;289:150–154 <https://doi.org/10.1006/bbrc.2001.5921>.
5. Tanner NA, Zhang Y, Evans TC, Jr. Visual detection of isothermal nucleic acid amplification using pH-sensitive dyes. *Biotechniques* 2015;58:59–68 <https://doi.org/10.2144/000114253>.
 6. Grimm JB, Brown TA, Tkachuk AN, Lavis LD. General synthetic method for Si-fluoresceins and Si-rhodamines. *ACS Cent Sci* 2017;3:975–985 <https://doi.org/10.1021/acscentsci.7b00247>.
 7. Grimm JB, Sung AJ, Legant WR, et al. Carbofluoresceins and carborhodamines as scaffolds for high-contrast fluorogenic probes. *Acs Chem Biol* 2013;8:1303–1310. <https://doi.org/10.1021/cb4000822>
 8. Zhang Y, Odiwuor N, Xiong J, et al. Rapid Molecular detection of SARS-CoV-2 (COVID-19) virus RNA using colorimetric LAMP. *Medrxiv*. 2020.02.26.20028373. <https://doi.org/10.1101/2020.02.26.20028373>
 9. Rabe BA, Cepko C. SARS-CoV-2 detection using isothermal amplification and a rapid, inexpensive protocol for sample inactivation and purification. *Proc Natl Acad Sci USA* 2020;117:24450–24458 <https://doi.org/10.1073/pnas.2011221117>.
 10. Wang D. One-pot detection of COVID-19 with real-time reverse-transcription loop-mediated isothermal amplification (RT-LAMP) assay and visual RT-LAMP assay. *Biorxiv*. 2020.04.21.052530. <https://doi.org/10.1101/2020.04.21.052530>
 11. Zhang Y, Ren G, Buss J, Barry AJ, Patton GC, Tanner NA. Enhancing colorimetric loop-mediated isothermal amplification speed and sensitivity with guanidine chloride. *Biotechniques* 2020;69:178–185 <https://doi.org/10.2144/btn-2020-0078>.
 12. Esposito S, Bosis S, Niesters HGM, Tremolati E, Begliatti E, Rognoni A, et al. Impact of human coronavirus infections in otherwise healthy children who attended an emergency department. *J Med Virol* 2006;78:1609–1615 <https://doi.org/10.1002/jmv.20745>.
 13. Uhteg K, Jarrett J, Richards M, Howard C, Morehead E, Geahr M, et al. Comparing the analytical performance of three SARS-CoV-2 molecular diagnostic assays. *J Clin Virol* 2020;127:104384 <https://doi.org/10.1016/j.jcv.2020.104384>.
 14. Mostafa HH, Lamson DM, Uhteg K, Geahr M, Gluck L, de Cárdenas JNB, et al. Multicenter evaluation of the NeuMoDx™ SARS-CoV-2 test. *J Clin Virol* 2020;130:104583 <https://doi.org/10.1016/j.jcv.2020.104583>.
 15. Lamb LE, Bartolone SN, Tree MO, Conway MJ, Rossignol J, Smith CP, et al. Rapid detection of Zika virus in urine samples and infected mosquitos by reverse-loop-mediated isothermal Amplification. *Sci Rep* 2018;8:3803 <https://doi.org/10.1038/s41598-018-22102-5>.
 16. Miyamoto S, Sano S, Takahashi K, Jikihara T. Method for colorimetric detection of double-stranded nucleic acid using leuco triphenylmethane dyes. *Anal Biochem* 2015;473:28–33 <https://doi.org/10.1016/j.ab.2014.12.016>.
 17. Tomita N, Mori Y, Kanda H, Notomi T. Loop-mediated isothermal amplification (LAMP) of gene sequences and simple visual detection of products. *Nat Protoc* 2008;3:877–882 <https://doi.org/10.1038/nprot.2008.57>.
 18. Goto M, Honda E, Ogura A, Nomoto A, Hanaki K. Colorimetric detection of loop-mediated isothermal amplification reaction by using hydroxy naphthol blue. *Biotechniques* 2009;46:167–172 <https://doi.org/10.2144/000113072>.
 19. Wang T, Lien C, Liu S, Selveraj P. Effective heat inactivation of SARS-CoV-2. *Medrxiv*. 2020.04.29.20085498. doi:<https://doi.org/10.1101/2020.04.29.20085498>
 20. Lalli MA, Chen X, Langmade SJ, et al. Rapid and extraction-free detection of SARS-CoV-2 from saliva with colorimetric LAMP. *Medrxiv*. 2020.05.07.20093542. doi:<https://doi.org/10.1101/2020.05.07.20093542>
 21. Lamb LE, Bartolone SN, Ward E, Chancellor MB. Rapid detection of novel coronavirus/Severe Acute Respiratory Syndrome Coronavirus 2 (SARS-CoV-2) by reverse transcription-loop-mediated isothermal amplification. *PLoS One* 2020;15:e0234682 <https://doi.org/10.1371/journal.pone.0234682>.
 22. Ben-Assa N, Naddaf R, Gefen T, Capucha T, Hajjo H, Mandelbaum N, et al. Direct on-the-spot detection of SARS-CoV-2 in patients. *Exp Biol Med (Maywood)* 2020;245:1187–1193 <https://doi.org/10.1177/1535370220941819>.
 23. Mohon AN, Hundt J, van Marle G, et al. Development and validation of direct RT-LAMP for SARS-CoV-2. *Medrxiv*. 2020.04.29.20075747. doi:<https://doi.org/10.1101/2020.04.29.20075747>
 24. Dao Thi VL, Herbst K, Boerner K, Meurer M, Kremer LP, Kirrmaier D, et al. A colorimetric RT-LAMP assay and LAMP-sequencing for detecting SARS-CoV-2 RNA in clinical samples. *Sci Transl Med* 2020;12:eabc7075 <https://doi.org/10.1126/scitranslmed.abc7075>.
 25. CDC. 2019. *Novel Coronavirus (2019-nCoV)*. Real-Time RT-PCR Diagnostic Panel
 26. Vogels CBF, Brito AF, Wyllie AL, et al. Analytical sensitivity and efficiency comparisons of SARS-COV-2 qRT-PCR primer-probe sets. *Medrxiv*. Published online 2020:2020.03.30.20048108. doi: <https://doi.org/10.1101/2020.03.30.20048108>
 27. Larremore DB, Wilder B, Lester E, et al. Test sensitivity is secondary to frequency and turnaround time for COVID-19 surveillance. *Medrxiv Prepr Serv Heal Sci*. Published online 2020. doi: <https://doi.org/10.1101/2020.06.22.20136309>
 28. Wyllie AL, Fournier J, Casanovas-Massana A, Campbell M, Tokuyama M, Vijayakumar P, et al. Saliva or nasopharyngeal swab specimens for detection of SARS-CoV-2. *N Engl J Med* 2020;383:1283–1286 <https://doi.org/10.1056/NEJMc2016359>.